BIOCHEMISTRY
including biophysical chemistry & molecular biology

Article

pubs.acs.org/biochemistry

Structure and Dynamics of Calmodulin (CaM) Bound to Nitric Oxide Synthase Peptides: Effects of a Phosphomimetic CaM Mutation

Michael Piazza, Kathryn Futrega, Donald E. Spratt, Thorsten Dieckmann,* and J. Guy Guillemette*

Department of Chemistry, University of Waterloo, Waterloo, Ontario N2L 3G1, Canada

Supporting Information

ABSTRACT: Nitric oxide synthase (NOS) plays a major role in a number of key physiological and pathological processes. Knowledge of how this is regulated is important. The small acidic calcium binding protein, calmodulin (CaM), is required to fully activate the enzyme. The exact mechanism of how CaM activates NOS is not fully understood. Studies have shown CaM to act like a switch that causes a conformational change in NOS to allow for the transfer of an electron between the reductase and oxygenase domains through a process that is thought to be highly dynamic. To investigate the dynamic properties of CaM–NOS interactions, we determined the solution structure of CaM bound to the inducible NOS (iNOS) and endothelial NOS (eNOS) CaM binding region peptides. In addition, we investigated the effect of CaM phosphorylation. Tyrosine 99 (Y99) of CaM is reported to be phosphorylated *in vivo*. We have produced a phosphomimetic Y99E CaM to investigate the structural and functional effects that the phosphorylation of this residue may have on nitric oxide production. All three mammalian NOS isoforms were included in the investigation. Our results show that a phosphomimetic Y99E CaM significantly reduces the maximal synthase activity of eNOS by 40% while having little effect on nNOS or iNOS activity. A comparative nuclear magnetic resonance study between phosphomimetic Y99E CaM and wild-type CaM bound to the eNOS CaM binding region peptide was performed. This investigation provides important insights into how the increased electronegativity of a phosphorylated CaM protein affects the binding, dynamics, and activation of the NOS enzymes.

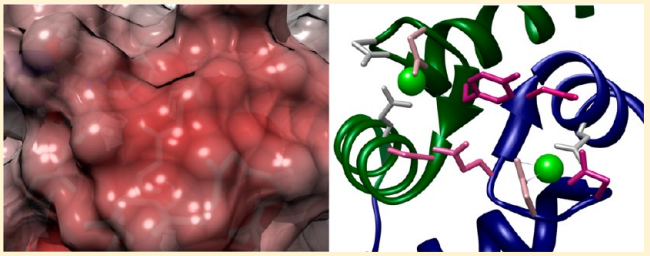

Calmodulin (CaM) is a ubiquitous cytosolic Ca^{2+}-binding protein that is able to bind and regulate hundreds of different intracellular proteins.[1] CaM consists of two globular domains joined by a flexible central linker region. Two EF hand pairs that are capable of binding to Ca^{2+} are found in each globular domain. The binding of Ca^{2+} to CaM causes the exposure of hydrophobic patches that allow it to associate with its intracellular target proteins. The flexibility of CaM's central linker separating the N- and C-domains allows it to adapt its conformation to optimally associate with its intracellular targets.[2] There is considerable interest in improving our understanding of the structural basis of CaM's ability to bind and recognize its numerous target proteins.

Among the target proteins bound and regulated by CaM are the nitric oxide synthase (NOS) enzymes (EC 1.14.13.39). These enzymes catalyze the production of nitric oxide ($^{\bullet}NO$) that acts as a secondary inter- and intracellular messenger involved in many physiological processes.[3] There are three NOS isozymes found in mammals: neuronal NOS (nNOS or NOS I), endothelial NOS (eNOS or NOS III), and inducible NOS (iNOS or NOS II). The NOS enzymes are homodimeric, with each monomer containing an N-terminal oxygenase domain and a C-terminal reductase domain. The oxygenase domain contains binding sites for the catalytic heme, tetrahydrobiopterin (H_4B), and the substrates L-arginine and molecular oxygen; the reductase domain contains binding sites for cofactors FMN, FAD, and NADPH. The oxygenase and reductase domains are connected by a CaM binding domain that is required for efficient transfer of an electron from the reductase to the oxygenase domain for $^{\bullet}NO$ production.[3,4] CaM binds and activates the Ca^{2+}-dependent constitutive NOS (cNOS) enzymes, eNOS and nNOS, at elevated cellular Ca^{2+} concentrations. In contrast, iNOS is controlled at the transcriptional level *in vivo* by cytokines and binds to CaM in a Ca^{2+}-independent manner. A conformational change that is associated with CaM binding is required for electron transfer within NOS enzymes.[5] The large conformational change that CaM induces in the reductase domain of the NOS enzymes allows the FMN domain to interact with the FAD to accept electrons and to pass the electrons to the heme during catalysis.[6] Clearly, these conformational changes caused by CaM are important in stimulating efficient electron transfer within the NOS enzymes.

There is considerable interest in understanding the structural basis of CaM's target protein interactions and diverse regulatory functions. It is well established that CaM is able to interact with its target enzymes in many different conformations.[1] For all three mammalian NOS isoforms, X-ray crystallographic and biophysical investigations indicate that CaM binds to peptides

Received: March 8, 2012
Revised: April 4, 2012
Published: April 9, 2012

encoding their CaM binding domain in an antiparalllel orientation and a collapsed conformation.[7]

It has become clear that a static view of protein structure is not sufficient to fully understand protein function.[8−10] The use of NMR allows information about the molecular dynamics of protein systems that cannot be obtained from a static image to be gathered. These studies provide direct evidence of structural changes and intramolecular dynamics associated with function that are central to gaining insights into the role of dynamics in protein function.[11−15] The approach of using an NMR study to complement a crystal structure has been demonstrated multiple times.[16−18]

This approach aids in correlating the static and dynamic picture of a structure and allows one to relate the two to function.[13] Using chemical shift changes, NMR spectroscopy is able to characterize at atomic (or residue) levels very weak interactions between proteins and ligands.[16,19] NMR spectroscopy also allows the study of a protein in its native environment instead of a crystal lattice, thereby providing structural information about disordered and flexible regions that cannot be obtained through crystallography.[11,19] An example of this is the solution structure of apo CaM, which revealed that the central linker was very flexible and the C-lobe adopts different conformations relative to the N-lobe because of this flexible linker.[20] This discovery was crucial in understanding the function of CaM as a calcium-dependent regulator.

Here we present the first systematic dynamics study of three CaM−NOS complexes, including two variants of NOS and one carrying a mutation simulating tyrosine phosphorylation. Even though the crystal structures are known, NMR assignments and structures were needed for studying the dynamics of this system. This lays the groundwork for future studies of these complexes.

EXPERIMENTAL PROCEDURES

Mutagenesis of CaM. The QuikChange site-directed mutagenesis procedure[21] was used to produce vectors encoding CaM Y99E and CaM Y99Q in the kanamycin resistant pET9dCaM plasmid.[22] The resulting vectors were confirmed by DNA sequencing.

Expression and Purification of CaM Protein. Wild-type CaM and mutant CaM proteins were expressed and purified using phenyl sepharose chromatography, as previously described.[22] Isolation of the CaM proteins (148 residues) was confirmed by ESI-MS, and the purity was judged to be >95% by sodium dodecyl sulfate−polyacrylamide gel electrophoresis. The human iNOS (RREIPLKVLVKAVLFACMLMRK, 22 residues corresponding to residues 510−531 from the full-length iNOS protein) and eNOS (TRKKTFKEVANAVKISASLMGT, 22 residues corresponding to residues 491−512 from the full-length eNOS protein) peptides were synthesized and purchased from Sigma, and their respective sequences are found in Table S3 of the Supporting Information.

Expression and Purification of NOS. Rat nNOS and bovine eNOS were expressed as previously described,[23,24] with the exception that these constructs had an N-terminal polyhistidine tail cloned upstream from their respective start codons. Human iNOS carrying a deletion of the first 70 amino acids and an N-terminal polyhistidine tail was coexpressed with wild-type CaM or the mutant CaM protein in *Escherichia coli* BL21(DE3) as previously described.[22] The purification of each NOS enzyme involved ammonium sulfate precipitation, metal chelation chromatography, and 2′,5′-ADP sepharose chromatography.[22]

Enzyme Kinetics. Electron transfer rates in the NOS enzymes were monitored using the NADPH oxidation, cytochrome *c* reduction, and the oxyhemoglobin capture assays, as previously described.[22−24] Assays were performed in 96-well microtiter plates in 100 μL total well volumes at 25 °C in a SpectraMax 384 Plus 96-well UV−visible spectrophotometer using Soft Max Pro (Molecular Devices, Sunnyvale, CA); 200 μM $CaCl_2$ or 250 μM EDTA and 3 μM wild-type or mutant CaM proteins were added to the appropriate samples. All assays were performed in quadruplicate on three different samples, and the 95% confidence interval is given.

Sample Preparation for NMR Investigation. Wild-type CaM and CaM Y99E for NMR experiments were expressed in M9 medium (11.03 g/L $Na_2HPO_4{\cdot}7H_2O$, 3.0 g/L KH_2PO_4, 0.5 g/L NaCl, 2 mM $MgSO_4$, 0.1 mM $CaCl_2$, 5 mg/mL thiamine, and 100 μg/mL kanamycin) containing 2 g/L [^{13}C]glucose and 1 g/L $^{15}NH_4Cl$. ^{13}C- and ^{15}N-labeled wild-type CaM and ^{15}N-labeled CaM Y99E were purified as described above. The samples were prepared for NMR experiments via buffer exchange into NMR buffer (100 mM KCl, 10 mM $CaCl_2$, 0.2 mM NaN_3, and a 90% H_2O/10% ^2H_2O mixture) at pH 6.0 using a YM10 centrifugal filter device (Millipore Corp., Billerica, MA). All NMR samples contained ≥1 mM wild-type CaM or CaM Y99E in a total volume of 500 μL. The samples were transferred into 5 mm NMR sample tubes and stored at 4 °C until they were required for NMR experiments. NMR experiments with the complexes were conducted on samples titrated with either iNOS or eNOS peptide to saturation in a 1:1 CaM:peptide ratio. Complex formation was monitored after each addition by acquisition of a ^{1}H−^{15}N heteronuclear single-quantum coherence (HSQC) spectrum. The isotope-labeled iNOS and eNOS peptides were prepared as previously reported.[25]

NMR Spectroscopy and Data Analysis. NMR spectra were recorded at 25 °C on Bruker 600 and 700 MHz DRX spectrometers equipped with XYZ-gradient triple-resonance probes (Bruker, Billerica, MA). Spectra were analyzed using CARA (Computer Aided Resonance Assignment).[26]

Specific assignments of the backbone resonances were achieved using a combination of three-dimensional triple-resonance experiments, including HNCA, HN(CO)CA, CBCA(CO)NH, and HNCO.[27,28] Side chain resonances were assigned using the TOCSY-type HC(C)H-TOCSY, (H)CCH-TOCSY, and H(CCO)NH experiments.[29]

Structure Calculation. The ^{1}H, ^{13}C, and ^{15}N resonance assignments were utilized to identify constraints for the structure calculations. For CaM and the iNOS peptide, these were obtained from ^{15}N NOESY-HSQC and ^{13}C NOESY-HSQC spectra.[30,31] In addition, dihedral angle restraints were derived from chemical shift analysis with TALOS+.[32] CNSsolve version 1.2[33] was used to perform the structure calculations using standard simulated annealing protocols. Constraints for the solution structure of the CaM−eNOS complex were derived from ^{15}N NOESY-HSQC and ^{13}C NOESY-HSQC spectra acquired on samples containing labeled CaM and unlabeled peptide. The peptide structure in this complex was modeled as an α-helix on the basis of previous structure studies[34] and positioned within the complex by the intermolecular NOEs identified in the NOESY spectra during the structure calculation. In addition, dihedral angle restraints from chemical shift analysis with TALOS+[32] were used for

Table 1. Statistics for the CaM−iNOS and CaM−eNOS Peptide Structural Ensemble

	CaM−iNOS complex			CaM−eNOS complex		
	CaM	iNOS	CaM-iNOS	CaM	eNOS	CaM-eNOS
NMR-Derived Distance and Dihedral Angle Restraints						
NOE constraints						
short-range ($\|i - j\| < 1$)	714	52	N/A	648	41[a]	N/A
sequential	956	92	N/A	750	84[a]	N/A
medium-range ($1 < \|i - j\| < 4$)	572	65	N/A	341	60[a]	N/A
long-range ($\|i - j\| > 4$)	237	1	99	239	0	43[b]
total	2480	210	99	1978	185[a]	43[b]
dihedral angles from TALOS+	266	14	N/A	270	14[a]	N/A
total no. of restraints		3069			2491[b]	
Structural Statistics for the 20 Lowest-Energy Structures						
mean deviation from ideal covalent geometry						
bond lengths (Å)		0.009			0.009	
bond angles (deg)		1.0			0.9	
average pairwise rmsd (Å) for all heavy atoms of the 20 lowest-energy structures	all	ordered[c]	selected[d]	all	ordered[e]	selected[f]
backbone atoms	0.8	0.7	0.7	1.2	1.1	1.1
heavy atoms	1.2	1.2	1.2	1.7	1.6	1.6
Ramachandran statistics (%)						
residues in the most favored region		90.5			89.8	
residues in additional allowed regions		7.9			10.0	
residues in the generously allowed region		1.7			0.1	
residues in the disallowed region		0.0			0.0	

[a]Modeled constraints. [b]Fewer restraints because of the unlabeled eNOS peptide. [c]Ordered residue ranges: 3A−147A and 150B−164B. [d]Selected residue ranges: 3A−147A and 150B−164B. [e]Ordered residue ranges: 3A−41A, 43A−55A, 57A−78A, 80A−114A, 117A−147A, and 152B−164B. [f]Selected residue ranges: 3A−41A, 43A−55A, 57A−78A, 80A−114A, 117A−147A, and 152B−164B.

CaM, along with secondary structure-based helical dihedral angles for the peptide.

Model of the CaM Y99E−eNOS Peptide. The model of the CaM Y99E−eNOS peptide was calculated like that of the CaM−eNOS peptide using CNSsolve version 1.2.[33] The calculation used the structural constraints input in the calculation of the structure of the CaM−eNOS peptide, except that the atoms of glutamate were substituted for those of Y99. All restraints involving the backbone atoms of Y99 were left in the input data as constraints for the backbone atoms of glutamate, whereas all constraints involving the side chain atoms of Y99 were removed. The average of the 20 lowest-energy structures was used for the model of the structure of the CaM Y99E−eNOS peptide.

DelPhi Calculation of the CaM Structures. DelPhi electrostatic potentials of the CaM−eNOS and CaM Y99E−eNOS structures were calculated using the DelPhiController interface of UCSF Chimera version 1.5.3 (build 33475).[35] The parseRes atomic radius file and atomic charge file were used as the input files in the calculation. The electrostatic potential surface was viewed in Chimera.

Accession Numbers. The "solution NMR structure of CaM bound to iNOS CaM binding domain peptide" has been assigned RCSB entry rcsb102516, Protein Data Bank (PDB) entry 2ll6, and BMRB accession number 18027. The "solution NMR structure of CaM bound to the eNOS CaM binding domain peptide" has been assigned RCSB entry rcsb102517, PDB entry 2ll7, and BMRB accession number 18028.

RESULTS AND DISCUSSION

The three-dimensional structures of different regions of NOS enzymes, but not the holoenzyme, have been determined by X-ray crystallography.[4] In several of the regions of interest, electron density was absent or weak, an indication of it being crystallographically disordered and, by inference, flexible. These studies were not able to give a direct measure of that flexibility. In contrast, NMR solution structure studies can provide information about the dynamic regions of proteins. Because cytoplasmic proteins function in solution, it is crucial to obtain detailed information about their structure in solution. Furthermore, although protein solution structures are often quite similar to their crystal structures, there are examples in which they may be somewhat or completely different.[36] The latter case has been reported upon investigation of the backbone dynamics of CaM in solution.[37]

In this investigation, we determined the three-dimensional solution structures of CaM bound to the human iNOS and eNOS CaM binding elements. This was made feasible by the development of a novel expression and purification system that allows for the production of individually stable isotope-labeled aggregation prone proteins.[25]

Structure of the CaM−iNOS CaM Binding Peptide Complex. The three-dimensional solution structure of CaM bound to the human iNOS CaM binding domain peptide (CaM−iNOS) was determined using multidimensional heteronuclear NMR spectroscopy. The structure of the complex is based on a large number of experimental constraints and is well-defined. Structural statistics are listed in Table 1. The family of 20 final structures is shown in Figure 1a. Residues 1−12 at the N-terminus of the iNOS CaM binding region peptide were not included in the structure calculation because they could not be unambiguously assigned. This is likely due to this region being highly mobile and unstructured as was previously seen in the crystal structure determined by Xia et al.[38] These residues include part of the intein cleavage site and restriction enzyme cutting site from the peptide production[25] as well as residues 510−514 from the iNOS peptide.

dx.doi.org/10.1021/bi300327z | Biochemistry 2012, 51, 3651−3661

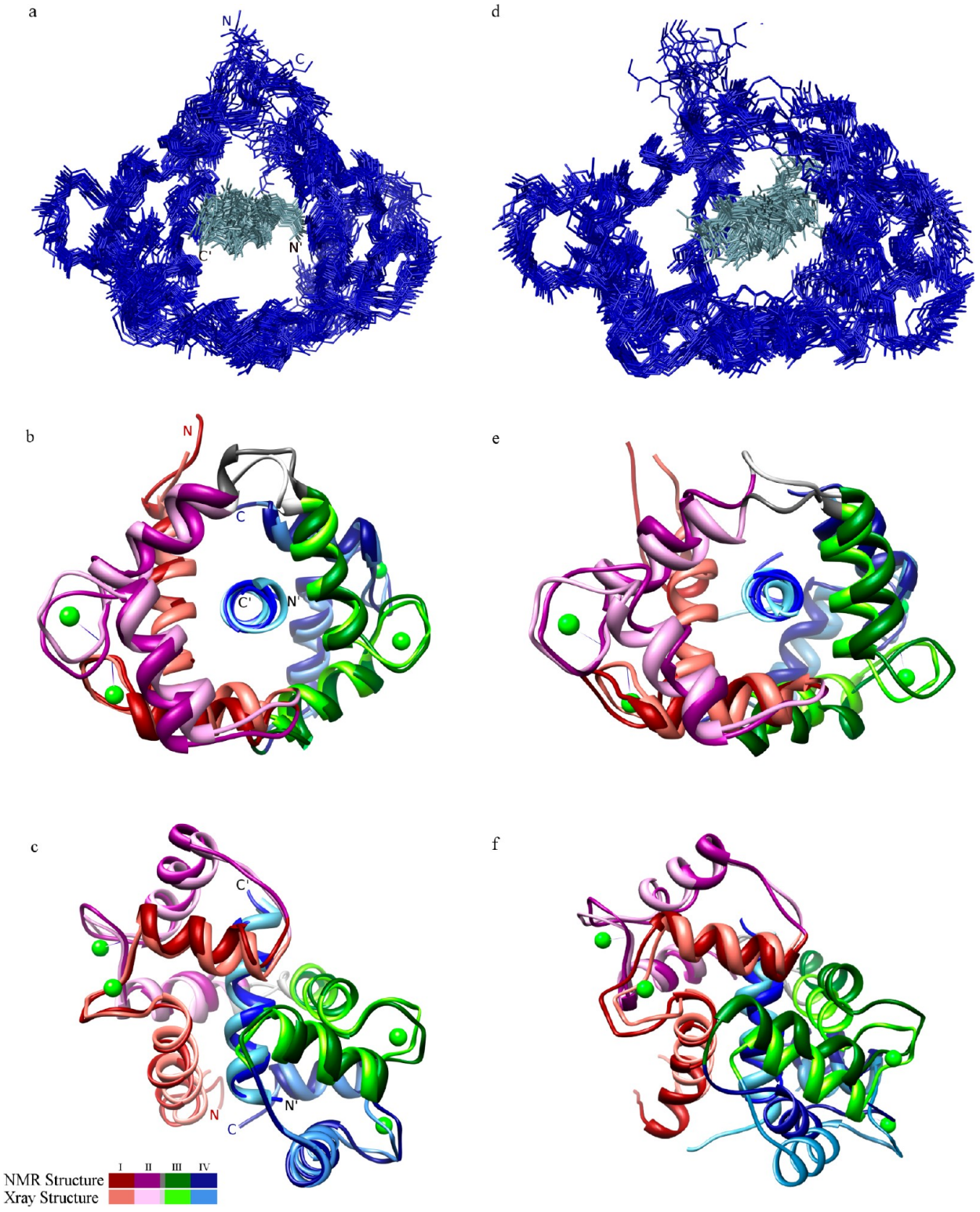

Figure 1. Solution structures of CaM bound to iNOS and eNOS CaM binding peptides. Superposition of the ensemble of the 20 lowest-energy calculated NMR solution structures of CaM bound to the iNOS peptide (a) and the eNOS peptide (d). Backbone atom traces of CaM are colored dark blue, and the iNOS peptide (a) and eNOS peptide (d) are colored light blue. Superpositions of the solution structures with the previously determined crystal structures of the CaM−iNOS (b and c) and CaM−eNOS (e and f) structures. Comparison of the solution structure of the CaM−iNOS peptide (dark colors) with the crystal structure (light colors) from PDB entry 3HR4 by superimposition of the two structures, viewed along the bound peptide from its C-terminus, front view (b), and rotated 90° with the C-terminus of the bound peptide on top, side view (c). Comparison of the solution structure of the CaM−eNOS peptide (dark colors) with the crystal structure (light colors) from PDB entry 1NIW by superimposition of the two structures, viewed along the bound peptide from its C-terminus (e) and rotated 90° with the C-terminus of the bound peptide on top (f). Residues 1−40 of CaM (EF hand I) are colored red, residues 41−79 (EF hand II) purple, residues 80−114 (EF hand III) green, and residues 115−148 (EF hand IV) blue. The peptide is colored lighter blue. Calcium ions from the crystal structure are shown as green spheres.

dx.doi.org/10.1021/bi300327z | *Biochemistry* 2012, 51, 3651−3661

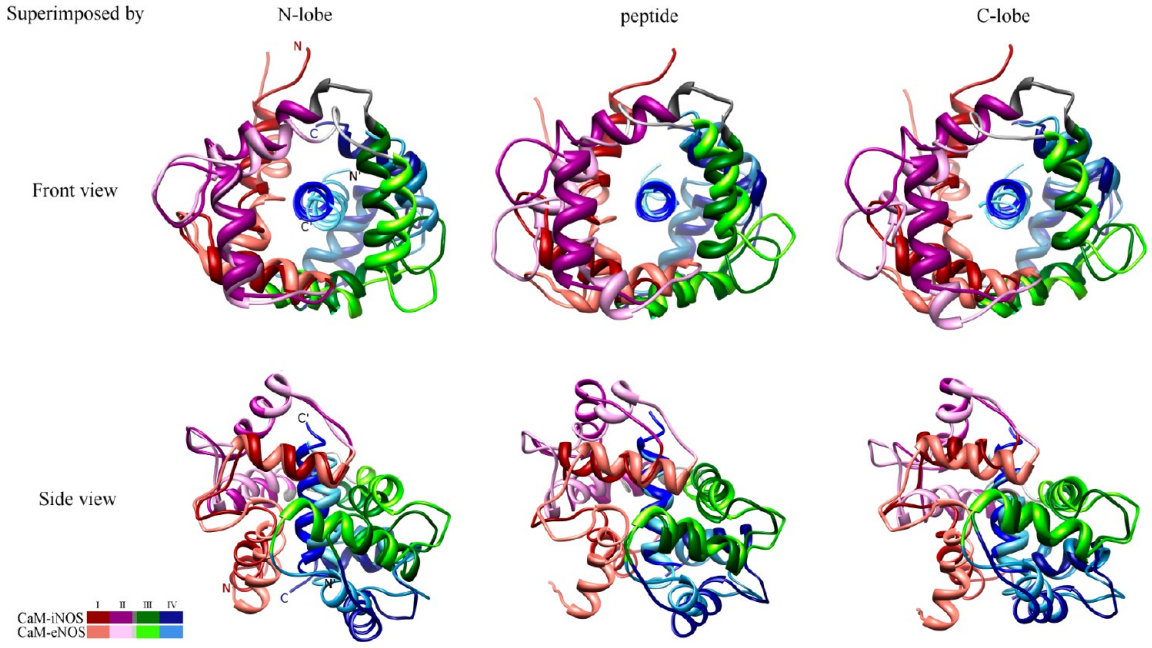

Figure 2. Superpositions of the CaM−iNOS peptide solution structure (dark colors) and the CaM−eNOS peptide solution structure (light colors). The two structures are aligned by superimposition of backbone atoms of the N-lobe of CaM (left column), the bound peptides (middle column), and the C-lobe of CaM (right column). The CaM−peptide complexes are viewed along the bound peptide helix from its C-terminus (C′) to its N-terminus (N′) in the top row (front view) and rotated 90° around the horizontal axis with the C-terminus of the bound peptide on the top in the bottom row (side view). The color scheme is the same as in Figure 1.

When the crystal (PDB entry 3HR4) and solution structures of the CaM−iNOS complex are superimposed (Figure 1b,c), the rmsd between the two backbones was found to be 1.5 Å for CaM and 1.1 Å for the iNOS peptide. There is a slight reorientation between the two structures in helices B and C (see Figure 5 for helix nomenclature), with the crystal structure having a closer packing of the helices than the bound peptide. Overall, the solution structure is quite similar to the previously reported crystal structure of the CaM−iNOS complex.

Structure of the CaM−eNOS CaM Binding Peptide Complex. The three-dimensional solution structure of CaM bound to the human eNOS CaM binding domain peptide (CaM−eNOS) was determined using multidimensional heteronuclear NMR spectroscopy. The structure is also well-defined as shown by superimposing the final 20 structures (Figure 1d). Structural statistics are listed in Table 1. The larger rmsd value for the family of CaM−eNOS structures compared to that of the CaM−iNOS structures is likely due to the smaller number of NOE constraints used in the structure calculation because of the lack of a sample with stable isotope-labeled eNOS.

When the crystal (PDB entry 1NIW) and solution structures of the CaM−eNOS complex were aligned (Figure 1e,f), an rmsd of 2.3 Å for the backbone atoms of CaM was found. Each of the lobes of CaM and the peptide individually superimpose well on each other. However, the relative orientation of the lobes with respect to each other and the peptide is less well-defined because of the smaller number of intermolecular NOEs. Nevertheless, the comparison with the crystal structure of the CaM−eNOS complex showed that the solution structure adopts the same overall conformation, and none of the NOEs we observed are in conflict with the crystal structure.

Comparison of the CaM−iNOS and CaM−eNOS Complexes. There are a number of studies indicating a stronger interaction exists between the iNOS peptide and CaM when compared to the association between the eNOS peptide and CaM. These studies have determined a K_d of 1.6 nM for the eNOS peptide and CaM and a K_d of <0.1 nM for the iNOS peptide and CaM. These studies have also shown that CaM binds to the eNOS peptide reversibly and that binding to the iNOS peptide is irreversible.[39−42]

When the solution structure of the CaM−iNOS complex was superimposed onto that of the CaM−eNOS complex, there were apparent differences in the relative orientations of the lobes (Figure 2). When aligned with respect to the backbone atoms of the N-lobe, the iNOS peptide is shifted closer to the N-lobe of CaM than the eNOS peptide, indicating that it is more tightly bound. This is consistent with results reported for the crystal structures of these two NOS isoforms.[34,38] There is also a difference in the orientation of helix A of CaM between the two structures, with helix A of the CaM−eNOS complex shifted toward the N-terminus of the eNOS peptide.

When the two structures are aligned with respect to the NOS peptide backbone atoms (Figure 2, middle structures), the C-lobes of the two CaM complexes are aligned closer to each other than the respective N-lobes. In comparison with the CaM−eNOS complex, the C-lobe of the CaM−iNOS complex is rotated clockwise, by ∼15°, around the peptide helix, and the N-lobe is rotated ∼30°. This suggests that the N-lobe of eNOS adopts a more open conformation, thereby exposing larger surface areas of the protein for interaction with CaM and its target protein. Our previous studies have shown that the N-lobe of CaM alone can activate iNOS to around 70% full activity while the C-lobe can stimulate the enzyme only ∼10% of that of wild-type CaM.[22] Neither of these two lobes on their own could stimulate the eNOS enzyme. In addition, repeated attempts failed to remove the N-lobe of CaM from the iNOS enzyme.[22,42] These results showing a tighter association of the N-lobe of CaM with the iNOS peptide when compared to the eNOS peptide further support the proposal that this lobe of CaM is principally responsible for the tighter binding of CaM.

dx.doi.org/10.1021/bi300327z | *Biochemistry* 2012, 51, 3651−3661

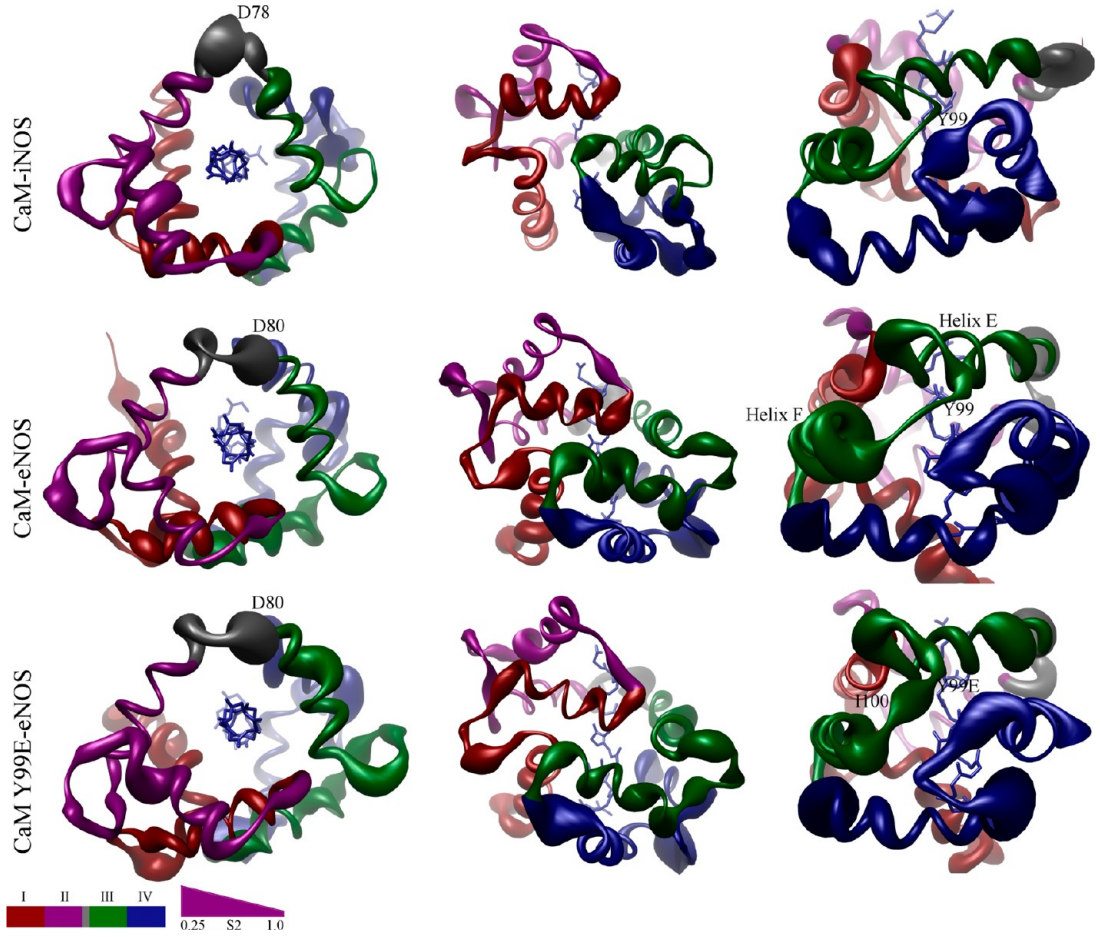

Figure 3. Worm models of CaM−iNOS peptide, CaM−eNOS peptide, and CaM Y99E−eNOS peptide complexes illustrating the intramolecular dynamics. The worm models were prepared using UCSF Chimera with the render by attribute function. The worm radius ranges from 0.25, corresponding to an S^2 value of 1, to 4, corresponding to an S^2 value of 0.25. The CaM−peptide complexes are viewed along the bound peptide helix from its C-terminus (front view) in the left column, rotated 90° around the horizontal axis with the C-terminus of the bound peptide on the top (side view) in the middle column, and looking at the interface of EF hands II and IV) in the right column. The bound peptide is shown in wire form. The color scheme is the same as in Figure 1.

The N-lobe of CaM forms a more stable structure with the iNOS peptide because of hydrophobic interactions. Several NOEs are found from helix C residues (Met51 and Val55) to Leu523 and helix D residues (Met72, Lys75, and Met76) to Met522 in the iNOS peptide. In contrast, the N-lobe has significantly fewer intermolecular NOEs from helix C and D residues to the eNOS peptide.

When aligned with respect to the backbone atoms of the C-lobe of CaM, helices E and F of the two CaM complexes are in slightly different conformations with respect to each other. In addition, one can see the same degree of rotation that was observed when the structures were aligned via the NOS peptide backbone atoms.

In all three views from Figure 2, the central linker regions (residues 77−81) of the two complexes are in different loop conformations. The CaM−eNOS linker region loop is more extended and resides closer to the helical peptide than the CaM−iNOS loop. This could in part account for the more open structure of the eNOS complex. The central linker of the CaM−eNOS structure is elongated when compared to that of the CaM−iNOS structure, having residues 75 and 76 being unwound from helix D. The linker region of the CaM−iNOS complex also has a higher pitch than that of the CaM−eNOS complex, because of the strong hydrophobic interactions of helices C and D with the iNOS peptide.

Conformational Dynamics of CaM−iNOS and CaM−eNOS Peptide Complexes. The difference in the relative strength of the interactions between CaM and the two target peptides used in this study was investigated by measuring the relaxation properties of the backbone ^{15}N nuclei in CaM. T_1, T_2, and $^1H-^{15}N$ NOE values were measured (see Tables S5 and S6 of the Supporting Information). The standard model free approach[43] was used to determine order parameters (S^2) for each of the CaM−peptide complexes, and the results are summarized in Figure 3. The two complexes have similar overall characteristics. The binding of CaM to the peptide causes the linker region to adopt a conformation more rigid than free CaM as illustrated by the higher S^2 values. This has also been in seen in other relaxation studies with CaM complexes.[44] Both the N-lobes and central linker regions of the two complexes show similar moderate order parameters. In contrast, when compared to the iNOS complex, the C-lobe of CaM in the eNOS complex has a higher degree of mobility (smaller S^2 values), especially for the residues in EF hand III. This is consistent with the weaker association of the eNOS peptide observed upon comparison of the CaM−iNOS and CaM−eNOS complexes. This can be attributed to the fact that

Table 2. Mutant CaM Protein Activation of iNOS[a]

		NADPH oxidation		Cyt *c* reduction		•NO synthesis		
		200 μM $CaCl_2$	250 μM EDTA	200 μM $CaCl_2$	250 μM EDTA	200 μM $CaCl_2$	250 μM EDTA	250 μM EDTA with 3 μM CaM
CaM	CaM	100 ± 2%	86 ± 4%	100 ± 4%	84 ± 5%	100 ± 4%	87 ± 2%	82 ± 2%
CaM Y99E	CaM Y99E	112 ± 7%	92 ± 3%	120 ± 4%	108 ± 5%	116 ± 4%	90 ± 3%	121 ± 3%
CaM Y99Q	CaM Y99Q	104 ± 4%	90 ± 4%	110 ± 4%	102 ± 5%	108 ± 4%	91 ± 2%	109 ± 4%

[a]•NO synthesis, cytochrome *c* reduction, and NADPH oxidation rates were measured with no exogenous CaM added to the assay. Each assay was performed in the presence of either 200 μM $CaCl_2$ or 250 μM EDTA as indicated. The activities obtained for iNOS coexpressed with CaM and assayed in the presence of 200 μM $CaCl_2$ at 25 °C were all set to 100% and were 52 min^{-1} (•NO synthesis), 83 min^{-1} (NADPH oxidation), and 1490 min^{-1} (cytochrome *c* reduction).

Table 3. Mutant CaM Protein Activation of cNOS Enzymes[a]

	neuronal NOS			endothelial NOS		
	NADPH oxidation	cytochrome *c* reduction	•NO production	NADPH oxidation	cytochrome *c* reduction	•NO synthesis
CaM	100 ± 4%	100 ± 3%	100 ± 2%	100 ± 1%	100 ± 4%	100 ± 2%
CaM Y99E	101 ± 5%	98 ± 3%	104 ± 3%	81 ± 5%	104 ± 4%	60 ± 3%
CaM Y99Q	93 ± 5%	95 ± 5%	110 ± 4%	91 ± 3%	94 ± 5%	82 ± 4%

[a]The oxyhemoglobin capture assay used to measure the rate of CaM-activated •NO production, the cytochrome *c* assay, and the NADPH oxidation assay were performed in the presence of either 3 μM wild-type or mutant CaM protein and either 200 μM $CaCl_2$ or 250 μM EDTA, as indicated. The activities obtained with the respective enzyme bound to wild-type CaM at 25 °C in the presence of 200 μM $CaCl_2$ were all set to 100%. The activities for nNOS bound to CaM were 35 min^{-1} (•NO synthesis), 130 min^{-1} (NADPH oxidation), and 1240 min^{-1} (cytochrome *c* reduction). The activities for eNOS bound to CaM were 8 min^{-1} (•NO synthesis), 25 min^{-1} (NADPH oxidation), and 68 min^{-1} (cytochrome *c* reduction).

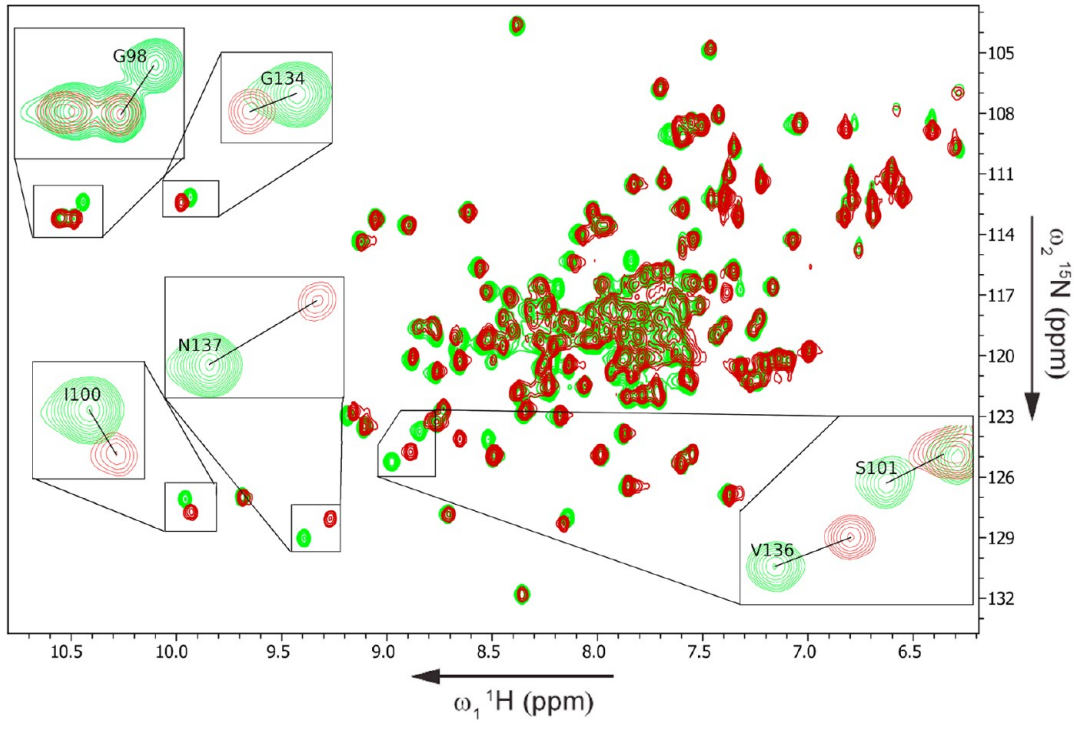

Figure 4. Overlay of $^1H-^{15}N$ HSQC spectra of the CaM–eNOS peptide complex (green) and the CaM Y99E–eNOS peptide complex (red). The insets of the overlay of the spectra show representative amide resonances for residues in EF hands III and IV that are affected by the mutation of Tyr99.

the iNOS peptide has more hydrophobic residues than the eNOS peptide, which form stronger interactions with the hydrophobic core of CaM.

Phosphomimetic Mutation of the CaM Y99 Residue. NMR spectroscopy has been shown to be a good method for investigating the structural effects of protein modification.[45] The interaction of CaM with its target proteins is modified by a number of post-translational modifications, including phosphorylation.[46] For example, of the 18 amino acid residues in CaM that have been proposed as candidates for phosphorylation, only eight have been verified to undergo this process by known kinases.[47] Four tyrosine kinases are known to phosphorylate tyrosine 99 in CaM. Phosphorylation of CaM residue Y99 has been reported to affect the CaM-dependent activity of a number of enzymes, including the NOS enzymes.[48,49] Studies of central nervous tissue hypoxia in

dx.doi.org/10.1021/bi300327z | *Biochemistry* 2012, 51, 3651–3661

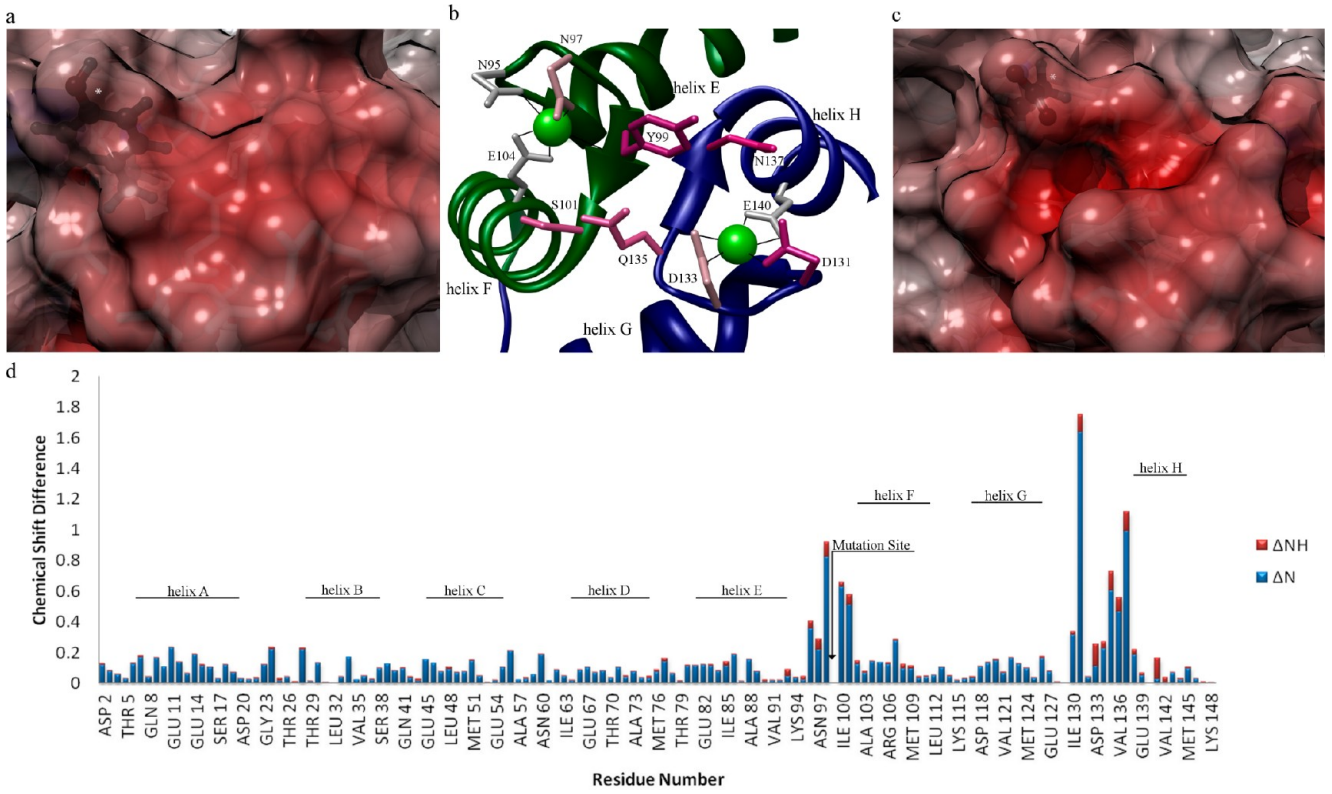

Figure 5. Mutation of Tyr99 affects the conformation of EF hands III and IV. The DelPhi-calculated electrostatic potential maps are projected on the surface of the solution structure of the CaM–eNOS peptide complex (a) and the calculated model of the CaM Y99E–eNOS peptide complex (c). Y99 and Y99E are denoted in the top left quadrant with asterisks. The DelPhi-calculated electrostatic potential maps are colored with a chimera color key ranging from red (−16) to blue (2). (b) Residues of the CaM–eNOS complex that have amide chemical shift differences of >0.25. The side chains of these residues are colored from light pink to dark pink, corresponding to the increase in the chemical shift difference. The color scheme is the same as in Figure 1. (d) Chemical shift differences between the native CaM–eNOS complex and the CaM Y99E–eNOS complex. The greatest differences are localized to Ca^{2+} binding loops of EF hands III and IV.

newborn piglets indicated that phosphorylation of Y99 of CaM affects the activity of endogenous NOS *in vivo*.[49] To assess the potential of NMR structural studies when investigating post-translational modifications of proteins, we decided to study the consequences of the phosphorylation of CaM Y99. A comparative investigation was performed on the effect that phosphorylation of this residue has upon the function of all three mammalian NOS isozymes. To allow the structural studies to be performed, a phosphomimetic form of CaM carrying a glutamate residue at position 99 (CaM Y99E) was used in the investigation. Phosphomimetic mutants have been used extensively for the investigation of protein phosphorylation.[50−54] The use of the phosphomimetic mutant in our investigation allowed the straightforward generation of isotopically labeled CaM for structural characterization without the difficulty of producing a specifically phosphorylated, isotope-labeled CaM. A second mutant in which tyrosine was replaced with glutamine (Y99Q) was also generated as a control.

CaM binding to NOS enzymes promotes electrons originating from NADPH to be transferred through the reductase domain to the catalytic heme of the adjacent NOS monomer's oxygenase domain.[7] There are three basic steps that make up the catalytic cycle of the reductase domain: (1) the transfer of the hydride from NADPH to FAD, (2) the transfer of an electron from FAD to FMN, and (3) the transfer of an electron from FMN to heme. These three steps can be monitored using NADPH oxidation, cytochrome *c*, and oxyhemoglobin capture assays, respectively, as previously described.[55] Each of these electron transfer steps has been shown to be dependent upon the dynamic properties of CaM and the conformational changes that CaM causes in the NOS enzymes.

The effect of the mutations on CaM-dependent activation of all three isoforms of nitric oxide synthase was investigated (see Tables 2 and 3). Both iNOS and nNOS enzymes produce only a small increase in nitric oxide production rates when bound by either of the two mutant CaM proteins. Both enzymes also showed small changes in the rate of NADPH oxidation and cytochrome *c* reduction. These results indicated that the mutation had little effect on the apparent properties of the enzyme. The eNOS enzyme function was more susceptible to the phosphomimetic mutation showing a decrease of 40% in nitric oxide production while still maintaining the full capacity to reduce cytochrome *c*. This suggests that the transfer of electrons from the reductase to the oxidase domain of eNOS was most affected by the mutation. For this reason, we decided to further investigate the effect of the mutation by obtaining a model of the solution structure of CaM Y99E bound to the eNOS peptide.

NMR Spectra Indicate the Altered Structure of EF Hands III and IV in the CaM Y99E–eNOS Complex. NMR spectroscopy was used to assess changes to the CaM–eNOS complex due to the mutation of Y99 to Glu. Figure 4 shows the overlay of the ^{15}N HSQC spectra of the CaM Y99E–eNOS complex with that of the CaM–eNOS complex. Cross-peaks for amides in the N-domain of CaM Y99E overlap with those of

dx.doi.org/10.1021/bi300327z | *Biochemistry* 2012, 51, 3651−3661

CaM, but amides in the C-domain, specifically the amides of residues in EF hands III and IV, do not overlap with those of CaM Y99E because of differences in chemical shifts. Almost all of the residues that participate in coordinating the Ca^{2+} ion in EF hands III and IV (Table S4 of the Supporting Information) are affected by changing Y99 to Glu.

Figure 5b shows why the mutation of Y99 to Glu would result in chemical shift differences seen in Figures 4 and 5d. Y99 contributes its carbonyl oxygen to the hydrogen bonding network used to stabilize the pentagonal bipyramidal coordination of the Ca^{2+} ion in EF hand III (Table S4 of the Supporting Information) and is also part of a β-strand that interacts with the β-strand of the EF hand IV loop. A substitution of Y99 with Glu would introduce a charge that could cause an electrostatic repulsion between the side chain of Glu and the carbonyl oxygen of V136 or N137. These residues are also involved in coordinating the Ca^{2+} ion in EF hand IV (Table S4 of the Supporting Information); therefore, any shift in their positioning should cause a perturbation in the other Ca^{2+}-coordinating residues of EF hand IV. This electrostatic repulsion should also cause the backbone of Y99 to be affected, which should perturb the tertiary geometry of the residues involved in coordinating the Ca^{2+} ion in EF hand III. This would account for the chemical shift changes observed in the overlaying of the ^{15}N HSQC spectra for the Ca^{2+}-coordinating residues of EF hands III and IV.

The introduction of a negative charge into this region due to the mutation would be expected to have structural effects on not only EF hand III but also EF hand IV. This is seen in the chemical shift differences between the wild-type and mutant forms of CaM bound to the eNOS peptide in Figure 5d. The analysis of our CaM Y99E model structure with DelPhi illustrates that the mutation causes a more negative potential on the surface of EF hand III (Figure 5a,c). This substitution causes a cleft to be formed on the surface of EF hand III. This is most likely due to the large aromatic group of Y99 being replaced with the less bulky side chain of Glu. This would likely not be present in the physiologically observed phosphorylated Y99. This change in the electrostatics on the surface of the protein would have a major effect upon the binding of CaM to its target proteins.

Consequences of the CaM Y99E Substitution on the Conformational Dynamics of the Complex. The order parameters (S^2) were determined for the CaM Y99E−eNOS peptide complex from ^{15}N relaxation data and compared with those of the native CaM complex as shown in Figure 3 and Table S3 of the Supporting Information. The substitution results in an increase in the dynamic motion of the central linker region. Residue 78 has the lowest S^2 value, thus demonstrating the highest internal dynamics in the linker region in the CaM−iNOS complex, whereas it is residue 80 in the CaM−eNOS and CaM Y99E−eNOS complexes that shows the highest degree of internal dynamics (Figure 3).

The Y99E substitution perturbs both EF hands III and IV, resulting in higher mobilities for most of the residues that are involved in Ca^{2+} coordination in both regions of the C-lobe of CaM. In EF hand III, this perturbation is especially large for residue 100 and other residues surrounding the bound Ca^{2+} ion, including residues in helix E, but not the dynamics of residues in helix F (Figure 3). The dynamic changes in EF hand IV associated with the Y99E substitution are mainly found in the linker region between helices G and H and reside closest to the mutation site in the three-dimensional structure of the protein (Figure 5b).

In summary, the NMR solution structures of both NOS peptides bound to CaM that were determined in this study are very similar to those of the previously reported X-ray crystallographic complexes. A direct comparison of the solution structures indicates that the N-lobe of the CaM−eNOS complex adopts a more open conformation and a greater surface area for interactions with its target protein. The structural studies indicate that the iNOS peptide forms a more stable complex with the N-lobe because of hydrophobic interactions. The conformational dynamics results show that the C-lobe of CaM in the eNOS−CaM complex has a higher degree of mobility. These results are consistent with the significantly higher affinity that exists between CaM and the iNOS CaM binding peptide.

The post-translational modification of CaM mimicked by replacement of a tyrosine with a glutamate within EF hand III showed only a significant decrease in the activity of the eNOS enzyme. The change in activity was associated with alterations in the structure and dynamics of the residues that coordinate the Ca^{2+} ions in both EF hands in the C-lobe of CaM. These observations provide important insights into our understanding of why eNOS enzymes require both lobes of CaM for activation while the iNOS enzyme is active when bound by only the N-lobe of CaM.

■ ASSOCIATED CONTENT

Supporting Information

Table of DNA oligonucleotides used, table of masses of CaM proteins, table of CaM binding peptide sequences, table of sequences of Ca^{2+} binding EF hands, tables of relaxation data for the CaM−NOS complexes, and the structure of a typical Ca^{2+} binding EF hand. This material is available free of charge via the Internet at http://pubs.acs.org.

■ AUTHOR INFORMATION

Corresponding Author

*Department of Chemistry, University of Waterloo, 200 University Ave. W., Waterloo, Ontario N2L 3G1, Canada. (T.D.) Telephone: (519) 888-4567, ext. 35036. Fax: (519) 746-0435. E-mail: tdieckma@uwaterloo.ca. (J.G.G.) Telephone: (519) 888-4567, ext. 35954. Fax: (519) 746-0435. E-mail: jguillem@uwaterloo.ca.

Funding

This work was supported, in whole or in part, by Discovery Grants held by J.G.G. and T.D. from the Natural Sciences and Engineering Research Council of Canada.

Notes

The authors declare no competing financial interest.

■ ACKNOWLEDGMENTS

Molecular graphics images were produced using the UCSF Chimera package from the Resource for Biocomputing, Visualization, and Informatics at the University of California, San Francisco (supported by National Institutes of Health Grant P41 RR001081). DelPhi is supported by funding from National Science Foundation Grant DBI-9904841.

■ ABBREVIATIONS

NOS, nitric oxide synthase; iNOS, inducible NOS; eNOS, endothelial NOS; nNOS, neuronal NOS; cNOS, constitutive

NOS; CaM, calmodulin; NMR, nuclear magnetic resonance; CaM−iNOS, CaM−iNOS binding domain peptide; CaM−eNOS, CaM−eNOS binding domain peptide; CaM Y99E−eNOS, CaM Y99E−eNOS binding domain peptide; PDB, Protein Data Bank; rmsd, root-mean-square deviation; NOE, nuclear Overhauser enhancement; NOESY, nuclear Overhauser effect spectroscopy; TOCSY, total correlation spectroscopy; HSQC, heteronuclear single-quantum coherence.

REFERENCES

(1) Ikura, M., and Ames, J. (2006) Genetic polymorphism and protein conformational plasticity in the calmodulin superfamily: Two ways to promote multifunctionality. *Proc. Natl. Acad. Sci. U.S.A. 103*, 1159−1164.

(2) Persechini, A., and Kretsinger, R. (1988) The central helix of calmodulin functions as a flexible tether. *J. Biol. Chem. 263*, 12175−12178.

(3) Alderton, W., Cooper, C., and Knowles, R. (2001) Nitric oxide synthases: Structure, function and inhibition. *Biochem. J. 357*, 593−615.

(4) Daff, S. (2010) NO synthase: Structures and mechanisms. *Nitric Oxide 23*, 1−11.

(5) Ghosh, D., and Salerno, J. (2003) Nitric Oxide Synthases: Domain structure and alignment in enzyme function and control. *Front. Biosci., 8*, D193−D209.

(6) Welland, A., and Daff, S. (2010) Conformation-dependent hydride transfer in neuronal nitric oxide synthase reductase domain. *FEBS J. 277*, 3833−3843.

(7) Spratt, D. E., Duangkham, Y., Taiakina, V., and Guillemette, J. G. (2011) Mapping the binding and CaM-dependent activation of NOS isozymes. *Open Nitric Oxide J. 3*, 16−24.

(8) Kohen, A., Cannio, R., Bartolucci, S., and Klinman, J. (1999) Enzyme dynamics and hydrogen tunnelling in a thermophilic alcohol dehydrogenase. *Nature 399*, 496−499.

(9) Brooks, C. L., Brünger, A., and Karplus, M. (1985) Active site dynamics in protein molecules: A stochastic boundary molecular-dynamics approach. *Biopolymers 24*, 843−865.

(10) Varley, P., and Pain, R. (1991) Relation between stability, dynamics and enzyme activity in 3-phosphoglycerate kinases from yeast and *Thermus thermophilus*. *J. Mol. Biol. 220*, 531−538.

(11) Kwan, A., Mobli, M., Gooley, P., King, G., and Mackay, J. (2011) Macromolecular NMR spectroscopy for the non-spectroscopist. *FEBS J. 278*, 687−703.

(12) Ishima, R., and Torchia, D. A. (2000) Protein dynamics from NMR. *Nat. Struct. Biol. 7*, 740−743.

(13) Kay, L. E. (1998) Protein dynamics from NMR. *Biochem. Cell Biol. 76*, 145−152.

(14) Kempf, J., and Loria, J. (2003) Protein dynamics from solution NMR: Theory and applications. *Cell Biochem. Biophys. 37*, 187−211.

(15) Wand, A. (2001) Dynamic activation of protein function: A view emerging from NMR spectroscopy. *Nat. Struct. Biol. 8*, 926−931.

(16) Pochapsky, T., Kazanis, S., and Dang, M. (2010) Conformational Plasticity and Structure/Function Relationships in Cytochromes P450. *Antioxid. Redox Signaling 13*, 1273−1296.

(17) Buck, M., Boyd, J., Redfield, C., MacKenzie, D. a., Jeenes, D. J., Archer, D. B., and Dobson, C. M. (1995) Structural determinants of protein dynamics: Analysis of ^{15}N NMR relaxation measurements for main-chain and side-chain nuclei of hen egg white lysozyme. *Biochemistry 34*, 4041−4055.

(18) Brunger, A. (1997) X-ray crystallography and NMR reveal complementary views of structure and dynamics. *Nat. Struct. Biol. 4*, 862−865.

(19) Sikic, K., Tomic, S., and Carugo, O. (2010) Systematic comparison of crystal and NMR protein structures deposited in the protein data bank. *Open Biochem. J. 4*, 83−95.

(20) Kuboniwa, H., Tjandra, N., Grzesiek, S., Ren, H., Klee, C. B., and Bax, A. (1995) Solution structure of calcium-free calmodulin. *Nat. Struct. Biol. 2*, 768−776.

(21) Wang, W., and Malcolm, B. (1999) Two-stage PCR protocol allowing introduction of multiple mutations, deletions and insertions using QuikChange site-directed mutagenesis. *BioTechniques 26*, 680−682.

(22) Spratt, D. E., Newman, E., Mosher, J., Ghosh, D., Salerno, J., and Guillemette, J. G. (2006) Binding and activation of nitric oxide synthase isozymes by calmodulin EF hand pairs. *FEBS J. 273*, 1759−1771.

(23) Montgomery, H. J., Romanov, V., and Guillemette, J. G. (2000) Removal of a putative inhibitory element reduces the calcium-dependent calmodulin activation of neuronal nitric-oxide synthase. *J. Biol. Chem. 275*, 5052−5058.

(24) Newman, E., Spratt, D. E., Mosher, J., Cheyne, B., Montgomery, H. J., Wilson, D., Weinberg, J., Smith, S., Salerno, J., Ghosh, D., and Guillemette, J. G. (2004) Differential activation of nitric-oxide synthase isozymes by calmodulin-troponin C chimeras. *J. Biol. Chem. 279*, 33547−33557.

(25) Piazza, M., Duangkham, Y., Spratt, D. E., Dieckmann, T., and Guillemette, J. G. (2011) Expression and purification of an isotopically labeled aggregation prone inducible nitric oxide synthase calmodulin-binding protein for use in nuclear magnetic resonance studies. *J. Labelled Compd. Radiopharm. 54*, 657−663.

(26) Keller, R. (2005) Optimizing the Process of Nuclear Magnetic Resonance Spectrum Analysis and Computer Aided Resonance Assignment. Thesis, Swiss Federal Institute of Technology, Zurich.

(27) Grzesiek, S., and Bax, A. (1992) Correlating Backbone Amide and Side Chain Resonances in Larger Proteins By Multiple Relayed Triple Resonance NMR. *J. Am. Chem. Soc. 114*, 6291−6293.

(28) Muhandiram, D. R., and Kay, L. E. (1994) Gradient-enhanced triple-resonance 3-dimensional NMR experiments with improved sensitivity. *J. Magn. Reson. 103*, 203−216.

(29) Bax, A., Clore, G. M., and Gronenborn, A. M. (1990) ^{1}H-^{1}H correlation via isotropic mixing of ^{13}C magnetization, a new three-dimensional approach for assigning ^{1}H and ^{13}C spectra of ^{13}C-enriched proteins. *J. Magn. Reson. 88*, 425−431.

(30) Clore, G. M., and Gronenborn, A. M. (1991) Applications of 3-dimensional and 4-dimensional heteronuclear NMR spectroscopy to protein structure determination. *Prog. Nucl. Magn. Reson. Spectrosc. 23*, 43−92.

(31) Fesik, S. W., and Zuiderweg, E. R. P. (1990) Heteronuclear 3-Dimensional NMR Spectroscopy of Isotopically Labelled Biological Macromolecules. *Q. Rev. Biophys. 23*, 97−131.

(32) Shen, Y., Delaglio, F., Cornilescu, G., and Bax, A. (2009) TALOS plus: A hybrid method for predicting protein backbone torsion angles from NMR chemical shifts. *J. Biomol. NMR 44*, 213−223.

(33) Brunger, A., Adams, P., Clore, G., DeLano, W., Gros, P., Grosse-Kunstleve, R., Jiang, J., Kuszewski, J., Nilges, M., Pannu, N., Read, R., Rice, L., Simonson, T., and Warren, G. (1998) Crystallography & NMR system: A new software suite for macromolecular structure determination. *Acta Crystallogr. D54*, 905−921.

(34) Aoyagi, M., Arvai, A., Tainer, J., and Getzoff, E. (2003) Structural basis for endothelial nitric oxide synthase binding to calmodulin. *EMBO J. 22*, 1234−1234.

(35) Pettersen, E. F., Goddard, T. D., Huang, C. C., Couch, G. S., Greenblatt, D. M., Meng, E. C., and Ferrin, T. E. (2004) UCSF chimera: A visualization system for exploratory research and analysis. *J. Comput. Chem. 25*, 1605−1612.

(36) Bertini, I., Kursula, P., Luchinat, C., Parigi, G., Vahokoski, J., Wilmanns, M., and Yuan, J. (2009) Accurate Solution Structures of Proteins from X-ray Data and a Minimal Set of NMR Data: Calmodulin-Peptide Complexes As Examples. *J. Am. Chem. Soc. 131*, 5134−5144.

(37) Barbato, G., Ikura, M., Kay, L. E., Pastor, R. W., and Bax, A. (1992) Backbone Dynamics of Calmodulin Studied by N-15 Relaxation Using Inverse Detected 2-Dimensional NMR Spectroscopy: The Central Helix Is Flexible. *Biochemistry 31*, 5269−5278.

(38) Xia, C., Misra, I., Iyanagi, T., and Kim, J. (2009) Regulation of Interdomain Interactions by Calmodulin in Inducible Nitric-oxide Synthase. *J. Biol. Chem. 284*, 30708−30717.
(39) Venema, R., Sayegh, H., Kent, J., and Harrison, D. (1996) Identification, characterization, and comparison of the calmodulin-binding domains of the endothelial and inducible nitric oxide synthases. *J. Biol. Chem. 271*, 6435−6440.
(40) Zoche, M., Bienert, M., Beyermann, M., and Koch, K. (1996) Distinct molecular recognition of calmodulin-binding sites in the neuronal and macrophage nitric oxide synthases: A surface plasmon resonance study. *Biochemistry 35*, 8742−8747.
(41) Wu, G., Berta, V., and Tsai, A. (2011) Binding kinetics of calmodulin with target peptides of three nitric oxide synthase isozymes. *J. Inorg. Biochem. 105*, 1226−1237.
(42) Spratt, D. E., Taiakina, V., Palmer, M., and Guillemette, J. G. (2007) Differential binding of calmodulin domains to constitutive and inducible nitric oxide synthase enzymes. *Biochemistry 46*, 8288−8300.
(43) Lipari, G., and Szabo, A. (1982) A model free approach to the interpretation of nuclear magnetic resonance relaxation in macromolecules. 1. Theory and range of validity. *J. Am. Chem. Soc. 104*, 4546−4559.
(44) Wang, T., Frederick, K., Igumenova, T., Wand, A., and Zuiderweg, E. (2005) Changes in calmodulin main-chain dynamics upon ligand binding revealed by cross-correlated NMR relaxation measurements. *J. Am. Chem. Soc. 127*, 828−829.
(45) Igumenova, T., Lee, A., and Wand, A. (2005) Backbone and side chain dynamics of mutant calmodulin-peptide complexes. *Biochemistry 44*, 12627−12639.
(46) Jang, D., Guo, M., and Wang, D. (2007) Proteomic and biochemical studies of calcium- and phosphorylation-dependent calmodulin complexes in mammalian cells. *J. Proteome Res. 6*, 3718−3728.
(47) Benaim, G., and Villalobo, A. (2002) Phosphorylation of calmodulin: Functional implications. *Eur. J. Biochem. 269*, 3619−3631.
(48) Corti, C., L'Hostis, E., Quadroni, M., Schmid, H., Durussel, I., Cox, J., Hatt, P., James, P., and Carafoli, E. (1999) Tyrosine phosphorylation modulates the interaction of calmodulin with its target proteins. *Eur. J. Biochem. 262*, 790−802.
(49) Mishra, O., Ashraf, Q., and Delivoria-Papadopoulos, M. (2009) Tyrosine phosphorylation of neuronal nitric oxide synthase (nNOS) during hypoxia in the cerebral cortex of newborn piglets: The role of nitric oxide. *Neurosci. Lett. 462*, 64−67.
(50) Greif, D., Sacks, D., and Michel, T. (2004) Calmodulin phosphorylation and modulation of endothelial nitric oxide synthase catalysis. *Proc. Natl. Acad. Sci. U.S.A. 101*, 1165−1170.
(51) Tran, Q., Leonard, J., Black, D., and Persechini, A. (2008) Phosphorylation within an autoinhibitory domain in endothelial nitric oxide synthase reduces the Ca^{2+} concentrations required for calmodulin to bind and activate the enzyme. *Biochemistry 47*, 7557−7566.
(52) Tran, Q., Leonard, J., Black, D., Nadeau, O., Boulatnikov, I., and Persechini, A. (2009) Effects of Combined Phosphorylation at Ser-617 and Ser-1179 in Endothelial Nitric-oxide Synthase on $EC_{50}^{Ca^{2+}}$ Values for Calmodulin Binding and Enzyme Activation. *J. Biol. Chem. 284*, 11892−11899.
(53) Garcia-Heredia, J., Diaz-Quintana, A., Salzano, M., Orzaez, M., Perez-Paya, E., Teixeira, M., De la Rosa, M., and Diaz-Moreno, I. (2011) Tyrosine phosphorylation turns alkaline transition into a biologically relevant process and makes human cytochrome c behave as an anti-apoptotic switch. *J. Biol. Inorg. Chem. 16*, 1155−1168.
(54) Guo, S., Burnette, R., Zhao, L., Vanderford, N., Poitout, V., Hagman, D., Henderson, E., Ozcan, S., Wadzinski, B., and Stein, R. (2009) The Stability and Transactivation Potential of the Mammalian MafA Transcription Factor Are Regulated by Serinei 65 Phosphorylation. *J. Biol. Chem. 284*, 759−765.
(55) Spratt, D. E., Israel, O., Taiakina, V., and Guillemette, J. G. (2008) Regulation of mammalian nitric oxide synthases by electrostatic interactions in the linker region of calmodulin. *Biochim. Biophys. Acta 1784*, 2065−2070.